1
Strategies to Improve the Accessibility to the Intracrystalline Void of Zeolite Materials: Some Chemical Reflections

Joaquín Pérez-Pariente and Teresa Álvaro-Muñoz

1.1
Introduction

Zeolites have been known for more than 250 years since the Swedish chemist and mineralogist Axel F. Cronstedt coined the term zeolite to baptize a new mineral that exhibited a very curious behavior when subjected to the action of a blowpipe [1, 2], for the mineral released substantial amount of water on heating, which it adsorbed again from the atmosphere on cooling without any noticeable change. The zeolite family of minerals introduced by Cronstedt consists of crystalline aluminosilicates formed by TO_4 tetrahedral units (T = Si, Al; Si/Al atom ratio not lower than 1) that are interconnected through the oxygen atoms to form tridimensional structures containing a large fraction of inner cavities of molecular dimension in which cations must be present in order to counterbalance the framework negative charge due to the presence of aluminum atoms. Moreover, the cations are hydrated. The presence of these cavities constitutes the key structural factor that differentiates zeolites from other related 3D tectosilicates, such as feldspars and it is indeed this factor that enabled these substances to occupy a privileged status in the modern chemical industry.

The scientific knowledge and technological development of zeolites have evolved enormously since their potential to perform selective adsorption of different compounds according to their molecular size was recognized in the 1930s [3]. This property of the zeolites to act as molecular sieves is attributed to the presence of pores of dimensions below 2 nm in the micropore structure that allow the reactants access to the inner cavities in such a way that only molecules smaller enough to enter through these pores are adsorbed, while the other molecules are excluded.

Prompted by the aforementioned discovery and with the increasing geological knowledge on zeolite formation in nature, efforts were made to obtain synthetic zeolites in the laboratory that can widen the field of application of the already known zeolite minerals. In this way, artificial specimens of zeolites that replicate the natural ones have been obtained, and, even more importantly, a large variety of zeolite structures without natural counterparts are synthesized every year, all

Mesoporous Zeolites: Preparation, Characterization and Applications, First Edition.
Edited by Javier García-Martínez and Kunhao Li.

around the world, to which it has to be added that new zeolite minerals are still being discovered [4].

By the time this chapter was written, 213 different zeolite structures had been discovered, and between six and seven new structures are added to the catalog every year. This evolution reflects not only a quantitative expansion of the field but also an ever-increasing growing of the chemical and structural complexity of these substances. Although this aspect is discussed in detail next, now it can be said that many zeolitic structures can only be composed of T atoms other than Si and Al, such as Ge, P, or Zn, in such a way that they are not aluminosilicates but aluminophosphates; or can contain just silicon and oxygen; or can be a combination of Ge, Si, and Al (in addition to oxygen) in several proportions. Mainly for this reason, the term *zeolite materials* is generally used to encompass microporous crystalline materials that have the basic structural features commonly and formerly attributed to zeolites, that is, to aluminosilicates. In this chapter, both the terms, zeolites and zeolite materials, are used indistinctly.

The application of zeolites in the chemical industry basically depends on two factors: the presence of appropriate active centers in the crystals and the architecture, size, and geometry of the inner cavities, which are responsible for the shape selectivity manifested by zeolite catalysts in a large number and variety of catalytic reactions. The active centers can be acid sites, associated with the presence of protons in the framework that compensate for the negative charge due to the trivalent elements tetrahedrally coordinated in the framework, such as Al^{3+}; redox-type cations such as Cr^{3+} or Co^{2+} that can replace some of the extraframework cations originally present in the structure; or some other elements that can replace the Si and/or Al of the framework. One of the most successful approaches of this type is the partial replacement of Ti for Si, which enables Ti-containing catalysts to oxidize a large variety of organic substrates selectively using hydrogen peroxide or organic peroxides as oxygen donors under mild conditions.

The active centers in zeolites can be located both in the inner cavities and at the external surface, and normally, they are present at both locations; however, it has to be considered that they could not be evenly distributed between the external surface and the internal surface of the crystals. This aspect is most relevant for the type of zeolite materials being dealt with in this chapter. Moreover, the presence of active sites in the zeolite micropores gives rise to shape-selective catalysis, which is a characteristic of this type of materials. The presence of micropores of molecular size imposes steric limitations to the diffusion of the reactants from the reaction media to the interior of the pores, and it prohibits the access of too bulky molecules. The same effect also reduces the diffusion rate of the reaction products outside the inner cavities. Moreover, the size and geometry of the inner cavities can also prevent the formation of certain reaction products, because the transition state required by the reaction mechanism cannot be accommodated in the space available in the micropores. In this way, a reaction pathway can be eventually favored among the several ones theoretically feasible on the basis of their respective steric requirements [5].

The two types of shape selectivity described in the first place, the ones based on the size of the reactants and products, are basically dependent on the diffusion length along the zeolite pores, and, for a given reactant, product, and zeolite, this selectivity is directly related to the crystal size along the diffusional path, that is, along the zeolite pores. However, the same properties of the zeolite crystals that produce such desirable shape-selective effects, namely, their shape and size, simultaneously reduce the accessibility of the reactants to the active sites and, hence, decrease the reaction rate, rendering a large portion of the actual zeolite crystals ineffective from the point of view of the catalyst. The reactants that are simply very bulky to penetrate the intricate pore system of the zeolites can only interact with the active sites located at the external surface.

These severe accessibility limitations can be overcome by following essentially three different yet complementary strategies. For the known zeolites that have already proven to be efficient catalysts, two different strategies can be followed. First, it is possible to reduce the crystal size, and eventually the shape, to decrease the diffusion effects along the pores. Second, it is possible to also reduce the diffusional path inside the pores by creating large pores (in some way, this means to create "cracks" or "holes" within the crystal bulk) in the crystals that facilitate the access of bulky molecules to a larger portion of the internal micropore system. The current catalytic cracking processes benefit from this approach, as such intracrystalline mesopores and also macropores have already been formed by the dealumination treatments of the zeolite catalysts, as it has been recognized long ago [6]. Finally, the last approach is the synthesis of new zeolite materials containing very large pores, which can be subjected to the same accessibility-increasing treatments as those applied to the existing zeolites.

All the previously described three main strategies have been experimentally implemented to enhance mass transportation in zeolite catalysts, and a large body of chemical literature has already been produced, which has been specifically cited in the following appropriate section. In the past 10 years, the second approach, the fabrication of mesopores (and, eventually, macropores) inside the zeolite crystals, has experienced revitalization thanks to the discovery of certain nanoengineering strategies that have brought much novelty to the field. In parallel to this, much attention has also been paid to the development of what are called *lamellar* zeolites, which are extremely structurally anisotropic zeolite materials, while new insights into the preparation of nanosized zeolite crystals have also been continuously reported, in addition to new exciting extra-large-pore materials. The relevance of all these aspects for catalytic applications has been discussed recently [7]. As excellent reviews on all of these aspects are already available to interested readers, several of them being published within a year or less this chapter has been in preparation, we do not intend to rereview what has already been reviewed. We have instead focused our work in a different direction.

As we had mentioned earlier, many of the most innovative approaches to synthesize zeolite materials with enhanced accessibility involve the creation of mesopores inside the zeolite crystals. For this reason, the term *mesopore zeolite* has

been coined. This term clearly describes the final physical property of the material from the point of view of the actual presence of mesopores in the crystals; however, it overshadows the chemical aspects that make possible the creation of such noncrystalline porosity within the crystals and the consequences that the physicochemical process that enables the formation of such pores might have on the chemical properties of the resulting materials. This field seems to be dominated by engineering approaches, more specifically nanoengineering, and we would like to highlight some of the chemical aspects we believe are required not only to understand the progress made until now but also, more importantly, to facilitate the improvement of the known methods or to serve as inspiration to develop new ones.

From the point of view of chemistry, several methods described so far to enhance the molecular accessibility to the intracrystalline voids of the zeolite materials can be classified according to the methodological tree presented in Scheme 1.1. The first distinction in the classification is made between the already existing zeolite structures and the strategies aiming at synthesizing new large-pore materials. The second main distinction is made between the methodologies that encompass the approaches to control the crystallization process

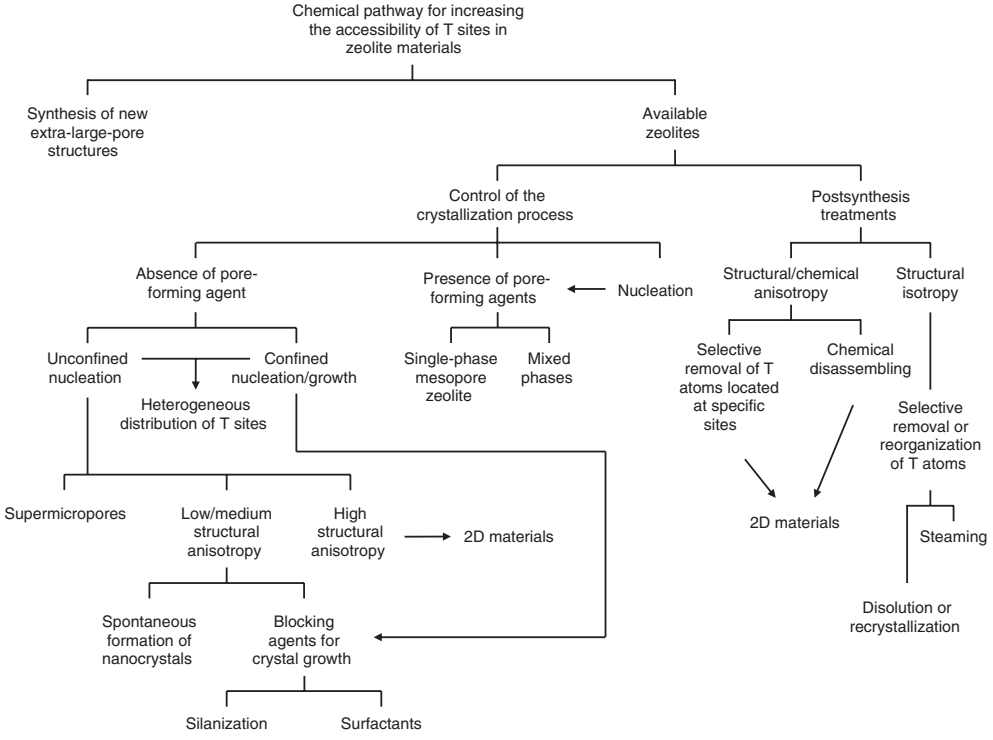

Scheme 1.1 Methods described to enhance the molecular accessibility to the intracrystalline voids of the zeolite materials.

of the zeolites, on the one hand, and the postsynthesis chemical treatments of the zeolites that involve, in some cases, partial recrystallization of the starting materials. Subsets of these categories are discussed in the following sections.

1.2 Strategies to Obtain New Large-Pore Materials

Zeolite materials are characterized by the presence of intracrystalline voids, which can adopt the geometry of channels, cavities, or, often, a combination of both. Access to these voids is limited by the aperture of the pores that project these voids on the external surface of the crystals. The size of the pore aperture is basically determined by the number of tetrahedral atoms forming the rings that delineate the pores, and by their shape, and the aperture size increases with that number. For the rings composed of 12 tetrahedral atoms, or 12-membered rings (12MRs) the largest pore aperture corresponds to the circular and coplanar rings, that is, all the T atoms are located on the same plane. This situation corresponds to materials having the faujasite structure with (FAU) code according to the classification of the International Zeolite Association (IZA) [8], which possesses a pore aperture of 7.4 Å. Out-of-plane configurations of T atoms, in the case of offretite, or elliptical rings, as those present in mordenite, always decrease the effective pore size. There are many examples of zeolite materials that contain inner cavities with a diameter greater than that of the pore aperture, or *window*, which allow the reactants access to these cavities, as the large supercage present in faujasite. Nevertheless, the pore aperture is always the limiting factor for the incoming molecules to penetrate into the zeolite crystal core, unless specific strategies are developed to expose these otherwise inaccessible cavities to the reactants, as it is discussed later. Therefore, one of the strongest driving forces of zeolite synthesis is the preparation of materials with the largest possible ring size, which would allow the access of bulky reactants to the intracrystalline cavities where most of the active centers are located. For this purpose, many different synthesis strategies have been developed over the years, involving a considerable material and intellectual effort made by many laboratories at both academic and industry [9] levels. On the basis of the accumulated experience, it is reasonable to evaluate the success of these synthesis approaches in tackling the target.

There are 213 available zeolite structures, and 71 of them possess at least 12MR or greater, about one-third of the total, which are known as *large-pore materials*. However, a vast majority of them are 12MR structures (Figure 1.1), and very few possess ring sizes above 12.

The uneven distribution of the rings according to their sizes is closely related to the concept of *framework density* (FD), which is defined as the number of T atoms per 1000 $Å^3$, a structural parameter that is commonly used to differentiate the zeolite structures from the other denser tectosilicates such as feldspars and several silica polymorphs. For nonzeolite frameworks, the FD values tend to be in the range 20–21. As the value of FD decreases for more open frameworks, the probability that the structure has large rings also increases. As can be seen in

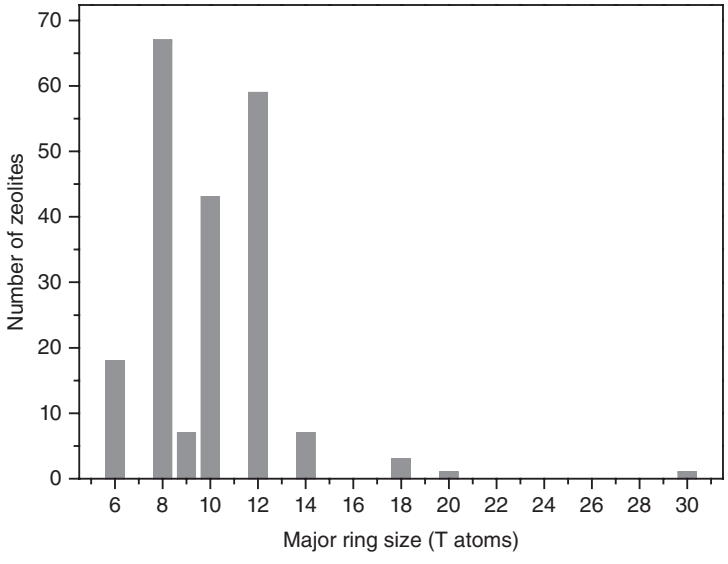

Figure 1.1 Number of the zeolite as a function of the major ring size.

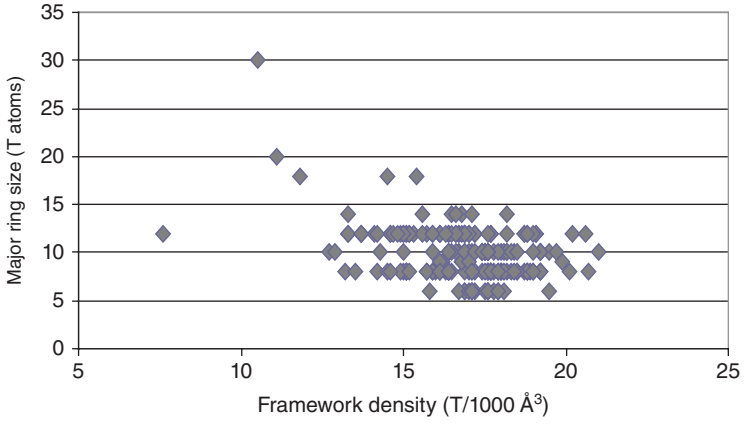

Figure 1.2 Number of the major ring size of the zeolite structure as a function of the framework density.

Figure 1.2, rings of sizes above 12 are only present in structures with low-FD values, about or below ~12, and, hence, this seems to be a criterion for the synthesis of such materials. However, the distribution of FDs among known zeolite structures shows a nonrandom specific pattern, which is presented in Figure 1.3. The distribution of zeolites as a function of their FD reaches a maximum at FD = 17, and there are very few structures with FD < 12.

Moreover, it is also interesting to plot the distribution of the FDs as a function of the time during which the structures of the corresponding zeolites were reported,

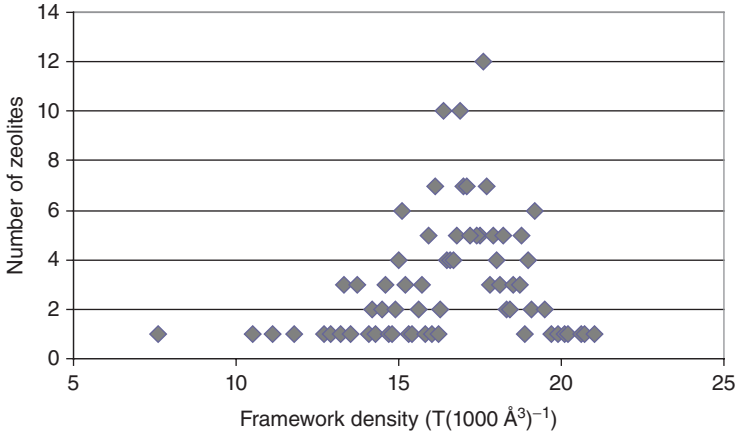

Figure 1.3 Number of the zeolite as a function of the framework density.

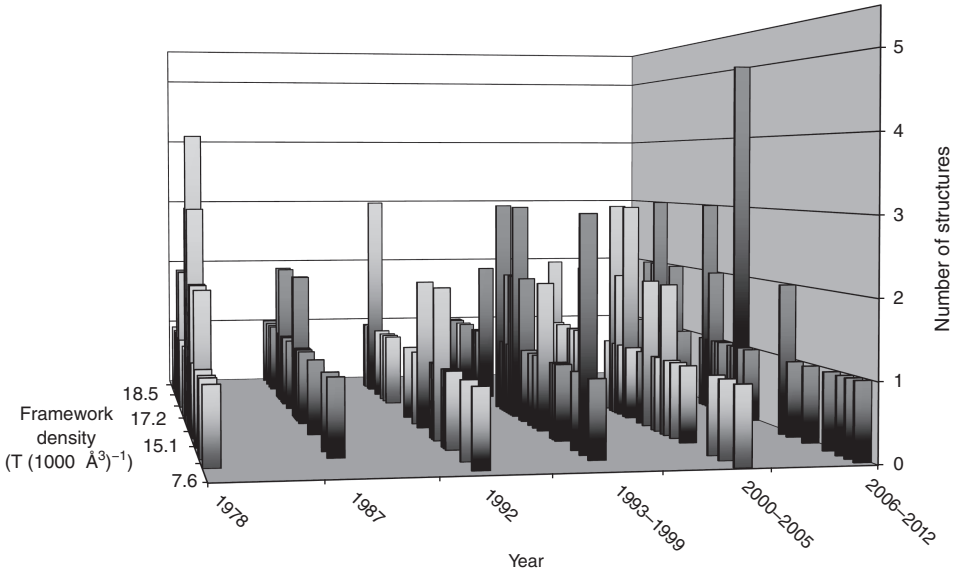

Figure 1.4 Distribution of the framework density as a function of the time.

as presented in Figure 1.4. In this way, the resulting graphic can be considered as an indication of the effectiveness of the synthesis efforts carried out in the past decades for obtaining large-pore materials, particularly those with ring sizes above 12. As mentioned earlier, specific synthesis strategies have been developed with the deliberate purpose of favoring the crystallization of hypothetical large-pore materials; therefore, they are not the result of random laboratory tests. The first set of data corresponds to the zeolites included in the first *Atlas of Zeolite Structures*

published by IZA in 1978. At that time, most of the structures corresponded to natural zeolites, and the distribution can be considered as a reference to the most favored FD in a geological environment. The distribution peaks at an FD value of ~17. In subsequent years, the relative weight of the artificial zeolite structures without natural counterparts significantly increased in such a way that the temporal distribution of FDs in the 1980s basically reflects the results of the laboratory work specifically designed to obtain large-pore structures. However, this distribution is still centered at quite the same value as compared to that of 1978, although the low-FD side of the distribution has been populated with some new and very interesting structures, particularly in recent years, as a result of innovative synthesis strategies, which are discussed next.

The data discussed previously can be considered as empirical evidence that zeolites having medium FD, in the narrow 16–18 range, are more stable as compared to those having lower or higher FD values. The reason for this behavior, in the case of such a maximum in the FD distribution, can be found as a combination of the following two opposite effects. On the one hand, the intrinsic stability of the zeolite frameworks increases with the FD. This can be manifested in the increase in the number of zeolite structures as the FD increases, which does not correspond to what has been empirically observed. As opposed to this effect, there exists a strong stabilizing interaction between the negatively charged framework and the hydrated cations located in the intracrystalline channels and cages. This effect increases as the FD reduces, because more space is available to accommodate these chemical species, and, hence, the overall contribution of this stabilizing interaction to the total zeolite energy increases. The final effect of such opposite trends is reflected in the maximum observed in the FD distribution, which suggests an optimum equilibrium of both effects at FD values in the range 16–18.

It is interesting to state that a connection between FD and the smallest ring in the loop configuration present in zeolite structures was proposed in Ref. [10]. According to this correlation, zeolites having a very low FD are expected to contain 3MR in their structure. Hence, the synthesis strategies that tend to favor the presence of such small rings increase the probability of obtaining large-pore materials. Moreover, the intrinsic framework stability of zeolite materials depends not only on the FD but also on their chemical composition. In this regard, it has been found that the D4Rs (double-four-membered rings) unit is stabilized by the incorporation of up to three Ge atoms [11], as compared with the pure-silicon version. Hence, the presence of such particularly stable SBUs (secondary building units) can contribute to the decrease in the overall framework energy, thereby favoring the crystallization of structures with a density lower than that attainable by pure-Si frameworks. This property has been used to synthesize several large-pore microporous germanosilicates with a low FD, most of which additionally contain three-ring units, as predicted in Ref. [10]. Some examples of this type of structure are ITQ-33, containing single 3MR and having an FD of 12.3 [12]; ITQ-44, also comprising a 18-ring structure and containing D3R, FD = 10.9 [13]; and ITQ-40, a 16-ring structure that has the lowest FD (10.1) among the already known zeolite structures [14].

It has been reported [15] that only 13 out of the 213 framework types available today are employed as catalysts for commercial purpose, and none of the structures synthesized over the past 20 years have found any application so far, to the best of our knowledge. Nevertheless, in that period, several new 12MR materials were obtained. Moreover, only five or six among those 13 frameworks are large-pore materials.

Considering all these aspects, it can be concluded that, although it is quite possible that large- and very-large-pore materials can find interesting commercial applications in some specific processes, there is a clear need to explore more general avenues to develop zeolite materials with enhanced pore accessibility.

1.3 Methodologies to Control the Crystallization Process of Zeolite Materials in the Absence of Pore-Forming Agents

A large number of these approaches involve control of the crystallization pathway of the zeolites using different strategies. Not all of them are reviewed here with the same amplitude; however, particular attention is paid to those that, in our view, have received comparatively less attention or are worthy of more in-depth study.

Probably the most simply way to reduce the diffusional constraints inside the zeolite intracrystalline pores is to reduce the length of the diffusional path, that is, to reduce the average crystal size (Figure 1.5). In addition, this strategy also increases the external surface area of the crystals in a substantial way, which can be very useful to process the molecules that are too bulky to diffuse inside the zeolite pores but can still react on the active sites located at the external surface. With

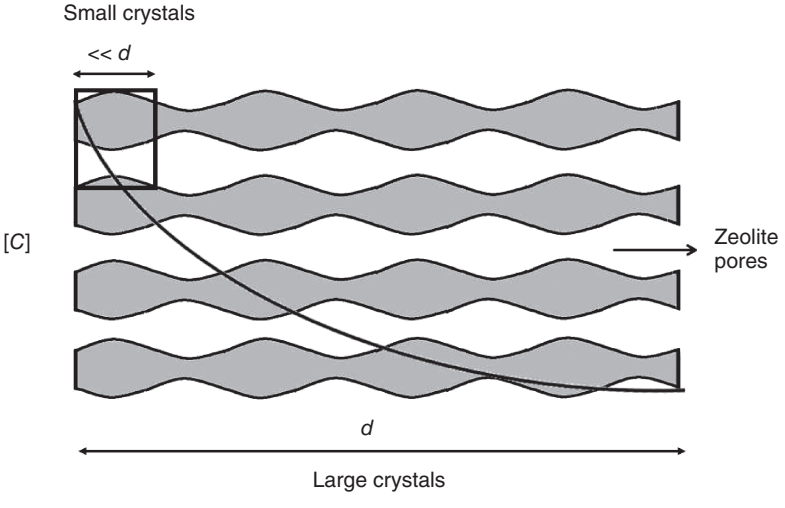

Figure 1.5 Schematic illustration of the diffusional constraints inside the zeolite with small or large crystal size.

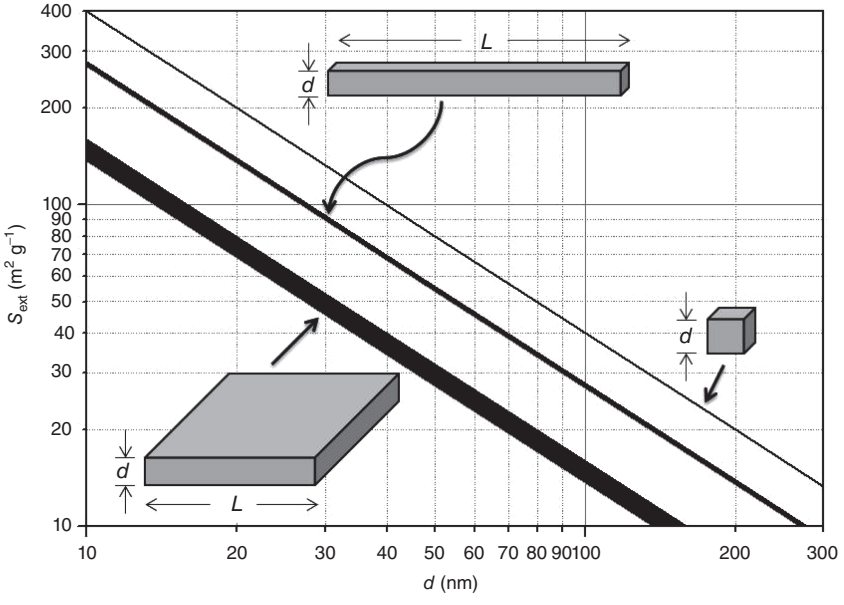

Figure 1.6 Variation of the external surface area of the zeolite nanoparticles with different shapes (cube, needle-like, and square plate) as a function of the crystal size. For needle-like and plates, the data are plotted as bands that indicate the surface area range corresponding to an aspect ratio *L*/*d* varying from 10 (upper limit) to 100 (lower limit), where *d* is the smallest particle dimension, that is, its thickness, and *L* is the plate side or needle length. The data have been calculated for a zeolite framework density of 17 T atoms per 1000 Å^3.

regard to the actual effect that the reduction of crystal size can have on the overall diffusion rate, it should be considered that many interesting zeolite structures are highly anisotropic from the point of view of their shape, which is, in general, a consequence of the large differences in the T atom densities in different crystallographic directions, which in turn reflect the existence of pores extending along a certain preferred crystal orientation. In this way, the zeolites containing monodirectional channels tend to adopt needle-shape morphologies in which the pores run along the main crystal axis.

The expected effect of the decrease in the average crystal size on the external surface area of the nanocrystals of zeolites has been plotted in Figure 1.6 for three different crystal shapes – cubes, needles, and plates – belonging to a model zeolite material that has an FD of 17. This value is representative of zeolites such as ZSM-5 with FD = 18.4 or mordenite with FD = 17. A flat surface has been assumed in every case, although real zeolite crystals do contain surface features (roughness, stepped surfaces, etc.) that can significantly increase the actual external surface area. However, this figure can still be useful to capture the crystal size–external surface area relationship in a semiquantitative manner. It can be seen that significant contribution of the external surface to the total area is expected only for zeolite crystals of size below 100 nm. For the cube-shaped morphology, crystals

of size about 30 nm exhibit an external surface area of about 100 $m^2 g^{-1}$. As the crystal shape becomes less isotropic, needles and plates, the crystal size required to reach that value is progressively reduced, and very thin platelets of thickness between 10 and 12 nm are required to obtain that external surface area. For pseudospherical crystals, the external surface area is smaller than that of the cubical ones with the same size. It is also interesting to mention that this simple model reflects that a large variation of the aspect ratio of the crystals, for example, the length-to-thickness ratio in plates, can have a slight influence on the external surface. This plot is referred to later when describing the textural properties of the so-called *mesopore zeolites.*

Several methodologies have been specifically developed to obtain nanosized zeolite crystals [16, 17]. However, under appropriate control of the nucleation step, ultrasmall crystals of a large-pore EMT zeolite, with sizes in the range 6–15 nm, have been obtained in the colloidal systems in the absence of any organic template [18]. The use of colloidal systems to obtain nanosized zeolite materials is not restricted to Si-based frameworks. Using this approach, SAPO-34 (silicoaluminophosphate) (carbonate-hydroxyapatite (CHA) structure) nanocrystals of size ~100 nm were obtained by microwave heating [19]. This latter result is particularly relevant to the catalysis, because of the recognized experimental difficulty in obtaining aluminophosphate-type materials in the submicrometer size.

1.3.1
Confined Nucleation and Growth

Appropriate control of the nucleation versus crystal growth rate allows for the synthesis of small zeolite crystals; however, in general, sizes below ~30 nm are not safely attainable, with a few exceptions, as described earlier. This is precisely the size range in which the contribution of the external surface to the total zeolite becomes significant. In order to achieve this goal, for the preparation of ultrasmall zeolite crystals, a different strategy was described by a series of papers by Jacobsen *et al.* [20–22], which the authors defined as *confined space synthesis.* This strategy is apparently very simple: it involves growing the zeolite inside the small pores present in an appropriate support. The size of the pores can impose a limitation to the crystal growth, and the nanocrystals formed in this way are recovered after removing the support. Several commercially available samples of carbon black were used as supports in these studies, which were removed after crystallization by calcination in air. Figure 1.7 shows a schematic representation of the final product.

Carbon black pearls BP700 and BP2000 were used in these experiments as confining matrices. In this way, and using BP2000, crystals of ZSM-5 with average crystal sizes in the range 20–75 nm were obtained, while those of Beta were in the range 7–30 nm; those of zeolite X were between 22 and 60 nm; and, finally, crystal sizes of zeolite A were in the range 25–37 nm. The textural properties of the carbon pearls are given in Ref. [21], and an average pore diameter of 45.6 nm is reported. Therefore, the crystal size is apparently controlled by the pore size

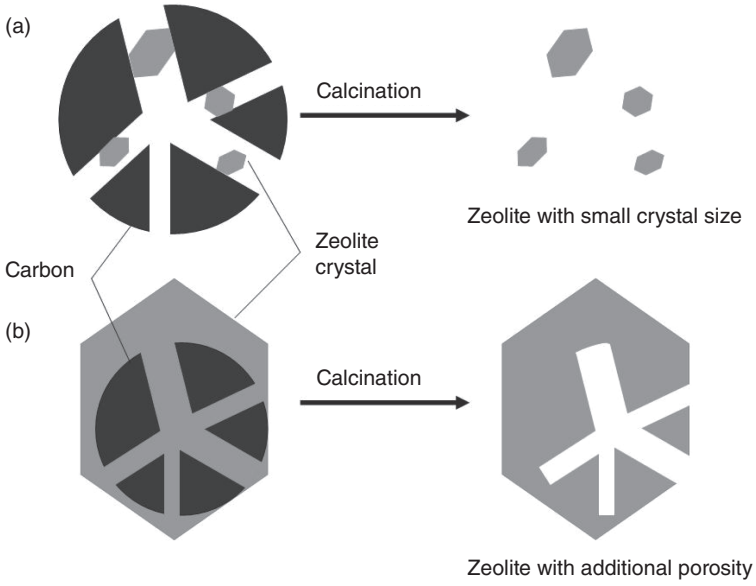

Figure 1.7 Schematic illustrations of (a) the *confined space synthesis* method to obtain nanocrystals and (b) the formation of an additional mesoporosity in the zeolite.

distribution of the matrix. However, it can be noticed that the carbon pore size is smaller than some of the aforementioned values for zeolite crystal size, which indicates some particle growth outside the carbon matrix. Moreover, a more careful inspection of further reports by the same group led to somewhat contradictory results. The particle size of BP2000 is 12 nm as reported in Ref. [23], a seminal paper that claimed the formation of mesopores inside the zeolite crystals using the same types of carbon black as pore-forming agents, an approach that is discussed next. Wang *et al.* [24] reported a particle size of 30 nm for this type of carbon black as determined by transmission electron microscopy (TEM) (averaging the sizes of only five particles, however), while most of the pores of this type of carbon black are below 5 nm as reported in Ref. [25]. Interestingly, the ZSM-5 crystals obtained by this method contain mesopores with an average radius of 17.5 nm and mesopore volumes in the range 0.5 – 1.0 ml g^{-1} [21]. Considering all these results , we ponder whether the ZSM-5 nanocrystals obtained by this method of confined space crystallization using carbon black matrices would have already formed small mesoporous zeolite crystals of the very same type as compared with those of larger size but also mesoporous, as reported in Ref. [23].

Another method to obtain more homogeneous ZSM-5 nanocrystals involves the use of colloid-imprinting carbons as matrices [26]. In this procedure, colloidal silica is used as an imprinting agent for a mesophase pitch used as carbon source. The resulting silica – carbon composite is washed with HF to remove the silica particles entrapped in the carbon matrix. Further, the resulting material is

impregnated with the synthesis solution in such a way that the zeolite crystallizes inside the carbon pores previously occupied by the silica nanoparticles. In this way, ZSM-5 nanocrystals in the range 13–90 nm were obtained.

1.3.2 Use of Blocking Agents for Crystal Growth

Other strategies that have been used to limit the crystal growth involve the use of certain chemical compounds that interact with the surface of the nanocrystals or protozeolitic nanounits present at the early stages of the nucleation process, in order to limit the crystal growth rate. Two approaches are discussed here: the silanization methods, on the one hand, and the addition of surfactants, on the other.

1.3.2.1 Silanization Methods

The silanization methods devised by Serrano *et al.*[27] involve several steps [28]. First, a synthesis gel is precrystallized to promote the formation of zeolitic seeds or protozeolitic units. Second, these units are functionalized by inducing their reaction with organosilanes. Further, the crystallization is continued in order to complete the zeolitization of the protozeolitic units. Finally, the sample is calcined in air to remove both the structure-directing agent and the organosilane. Several organotrialkoxysilanes can be used; however, phenylaminopropyltrimethoxysilane is preferred because it produces ultrasmall crystals in the range 5–10 nm, with a more uniform pore size distribution. Furthermore, 2D ^{29}Si (H) heteronuclear correlation (HETCOR) spectra of the as-made silanized nanocrystals show that the silane moieties are anchored to the external surface and not inside the pores [29]. A closely related strategy designed by Pinnavaia *et al.* [30, 31] involves the use of a silylated polymer that is grafted on the external surface of the protozeolitic units, which grow leaving behind the polymer encapsulated in the crystal aggregates, thereby forming mesopores after calcination.

The silanization method produces extremely small crystals, with the highest external surface areas ever reported, which are a function of the several synthesis parameters. In the case of ZSM-5, nanocrystals with an external surface area of about 500 $m^2 \cdot g^{-1}$ are obtained; however, the micropore area (and the micropore volume) decreases, in the same manner, to a value lower than 200 $m^2 \cdot g^{-1}$ for the samples with the highest external surface area. Conventional, micrometer-sized crystals of ZSM-5 have a micropore surface area of ~350 $m^2 \cdot g^{-1}$. According to the plot shown in Figure 1.6, such high values of external surface area cannot be solely explained by the decrease in the crystal size. There is a possibility that such values reflect the large contribution of the surface roughness produced at the termination of the crystal, as represented in Figure 1.8.

The noticeable yet less pronounced decrease in the micropore surface area, or the micropore volume, observed in the zeolite nanocrystals synthesized by other methods, also requires an explanation. First, this decrease can be just because the ratio between the structural micropore volume and the mass of zeolite, given by

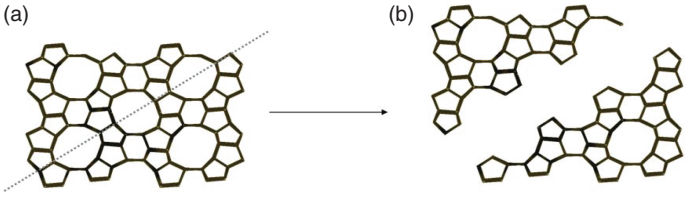

Figure 1.8 Illustration of the micropore channels of the MFI structure for crystals of different size.

the number and composition of the TO_2 units per unit cell, which can be calculated for quasi-infinite crystals of micrometer size for practical purposes, does not apply to ultrasmall crystals, as depicted in Figure 1.8.

Five micropore channels are represented in this projection of a small crystal with an MFI structure. When the crystal is halved along the dotted line, two smaller crystals of weight equivalent to that of the original (because the initial number of T units have been preserved) are obtained; however, both the crystals contain only one channel system each; therefore, three-fifth of the initial micropore volume (and, consequently, of the micropore surface) of the original larger crystal has been lost. Moreover, the surface roughness per unit weight has also increased significantly.

The extreme reduction of zeolites crystal size could also have other chemical consequences in addition to the geometry aspects discussed above. First, the fraction of external T sites as compared with the internal ones would be very much larger than those in the conventional crystals. Many of these T sites can be terminated by silanol (Si–OH) groups, which are hydrophilic. In this way, the hydrophobic/hydrophilic balance of the crystal would be highly affected by the extreme reduction of crystal size. Further, an all-silica framework, which usually exhibits a hydrophobic character in micrometer-sized crystals, such as MFI, would rather be hydrophilic for ultrasmall crystal specimens. Hence, this aspect could have consequences not only in the adsorption processes but also in catalysis, as it dramatically alters the adsorption equilibrium of the reactants and products as a function of their relative polarity.

In addition to this aspect, it should be also considered whether the zeolite nanocrystals, particularly the ultrasmall ones, still retain at their surface and their vicinity the chemical properties associated with the active sites located at the interior of the micron-sized crystals. In this regard, as pointed out earlier, the intrinsic stability of the zeolites is smaller than that in the denser phases or that of amorphous materials. Moreover, the free energy in the condensed phases at the surface is generally high, and it is compensated by the reticular energy only when the size of the crystal increases. This factor is very well known, and it practically occurs during the nucleation of the zeolitic phases in gels. For this reason, it is possible that, for nanocrystals, the structure of the external surface does not necessarily retain the local structure and, hence, the chemical properties commonly observed in large zeolite crystals. Indeed, this aspect offers an alternative explanation for the strong reduction of micropore volume

observed in ultrasmall crystals, because it is possible that, in addition to the effect described by the simple model represented in Figure 1.8, some portion of the crystals in the vicinity of the external surface collapse, that is, become amorphous and, therefore, do not exhibit any longer the regular crystalline arrangement of atoms present in the interior of the micropores [32]. The characterization of the surface properties of these ultrasmall crystals can be very useful to determine the extent to which they are affected by the extreme reduction of the crystal size. However, there is already some evidence that a considerable portion of the nanocrystals have already lost the chemical properties associated with the micrometer-sized ones after calcination.

It has been reported that the framework aluminum in the silanized samples is less stable when compared with the conventional ZSM-5 zeolite, as determined by ^{27}Al magic-angle spinning (MAS) NMR [33]. Moreover, ammonia desorption indicates that the acid concentration decreases as the mesopore/micropore surface area increases, that is, as the crystal size reduces [34], in agreement with the removal of framework aluminum, and the overall acid strength of the acid sites also decreases similarly. The content of the Brønsted acid sites determined by means of the Fourier transform infrared spectroscopy (FTIR) spectra of adsorbed pyridine also decreases in the silanized samples as compared with the conventional ones [33, 35]. Nevertheless, a positive finding is that these samples contain a large number of fairly strong Lewis acid sites [33]. All these results clearly indicate that the stability of the nanocrystals decreases rapidly with the crystal size, and this effect is quite significant for ultrasmall crystals of sizes in the range 5–10 nm.

Reduction of the zeolite micropore volume (and the surface area) concomitant with an increase in the mesopore surface area has already been recognized by Pérez-Ramirez *et al.* [36], not only in the silanization method but also in most of the procedures reported at that time to prepare zeolite materials with enhanced pore accessibility. These materials are also often termed *hierarchical zeolites*, in the context that they comprise, in addition to the intracrystalline structural micropores, exostructural mesopores and, eventually, macropores, thereby possessing a hierarchy of pores of different sizes. In this regard, the same group developed the concept of hierarchy factor (HF), which expresses the relationship between the relative micropore volume ($V_{\text{micro}}/V_{\text{total}}$) and the relative mesopore surface area (S_{mesop})/(S_{BET}). The objective of the methods used for successfully increasing the accessibility is to maximize the HF, which involves enhancing the mesopore surface without severely affecting the micropore volume.

It can be concluded from the aforementioned results of the silanization method that, for practical catalytic purposes, there is a compromise between the crystal size and stability, and excessively small nanocrystals are probably not the most preferred materials if enhancement of the accessibility to the micropores is required while the micropore volume needs to be preserved. Moreover, the optimum (nano)crystal size would be different for different zeolite materials.

1.3.2.2 Use of Surfactants in the Synthesis of Silicoaluminophosphates

The silanization method specifically designed to decrease the crystal size, though successful in this regard, also illustrates that the chemical properties of the active sites are also highly modified, not necessarily in the desired direction. This conclusion could most probably be extended to many other procedures designed to obtain zeolite materials with enhanced accessibility, and it should be considered in the evaluation of their suitability for specific catalytic purposes. One earlier example of this aspect, the unavoidable relationship between the chemical methods used to gain micropore accessibility and the impact that these methods can have on the chemical environment of the zeolite active sites, is concerned with the synthesis of crystalline microporous SAPOs in the presence of surfactants. There have been very few studies on these zeolite-type materials as compared with silicon-based structures with regard to accessibility-enhancing synthesis strategies, which probably reflect the comparatively lower impact of these materials at industrial scale in the catalysis field.

Pure aluminophosphate frameworks (AlPO) are neutral, similar to all-silicon zeolites, and further, active sites must be introduced in their structure for catalytic purposes. The replacement of P(V) by Si(IV) generates a negative charge in the framework that could be compensated by a proton, much in the same way when Si(IV) is replaced by Al(III) in a zeolite structure. However, there is also a possibility of simultaneous replacement of one P(V) + Al(III) pair by two Si(IV) atoms. The combination of these substitution mechanisms generates Si environments in the structure of the type $Si(Al_nSi_{4-n})$, where $n = 0 - 4$, leading to materials with different number and strength of acid sites. In an attempt to gain control over the silicon environment in the framework of silicon-substituted aluminophosphates, and, hence, on the catalytic properties of the resulting materials, in the late 1980s, Derouane *et al.* [37] designed a new synthesis strategy involving the use of two-liquid phases in the synthesis gel, as depicted in Figure 1.9.

This procedure involves the use of an alkoxysilane, for example, tetraethoxysilane (TEOS) as silicon source, which is dissolved in a solvent immiscible with water, such as *n*-hexanol. The P and Al sources are present in the aqueous phase in such a way that the TEOS is slowly hydrolyzed at the water–hexanol interface; its concentration in the aqueous phase remains low during crystallization. In this way, it was expected to replace mainly P(V), avoiding the substitution mechanism by pairs, which produces materials with a very low level of acidity.

This procedure was later modified by another group by introducing an amphiphilic agent that disperses the organic phase into the aqueous one by forming micelles, thereby producing a microemulsion. Long-chain trialkylammonium cations such as hexadecyl- and dodecyltrimethylammonium, long-chain alkylamines, and neutral amphiphilic molecules were used as surfactants. It was found that the presence of cationic and fatty amines in the two-liquid phase system has a significant influence both on the mechanism of Si incorporation in the crystals and on the textural properties of the resulting materials such as large-pore AFI structure [38, 39], extra-large-pore VFI [40], medium-pore AEL [41], and, more recently, small pore CHA-type material SAPO-34 [42]. Often,

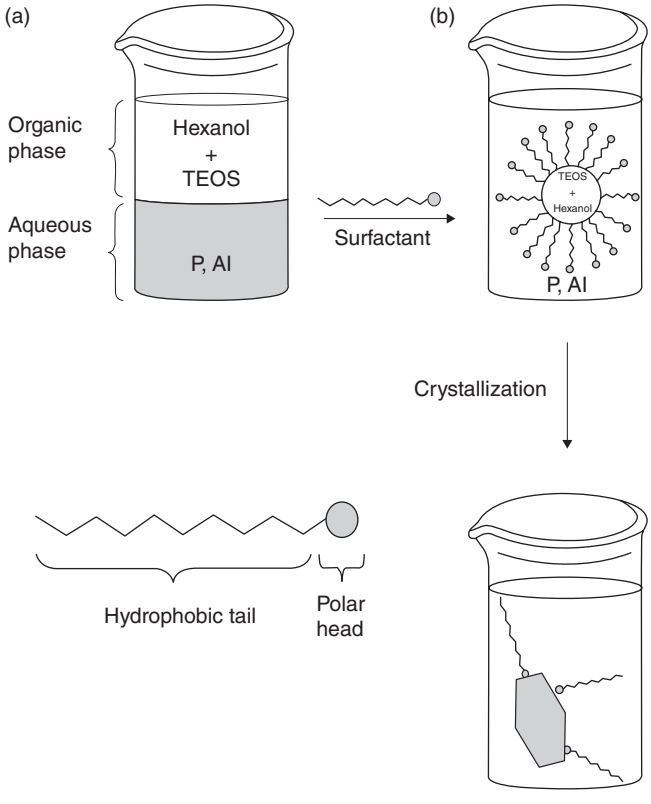

Figure 1.9 Schematic illustration of the synthesis strategy involving the use of two-liquid phases in the synthesis gel in the absence (a) and in the presence (b) of surfactant.

the as-made crystals synthesized by this method have been found to contain an excess of organic material as compared with the conventional reference material, which is due to the presence of the surfactant in the crystals. It has been found by ^{29}Si MAS NMR that the silicon substitution mechanism is modified in such a way that materials with higher total acidity and acid strength are obtained as compared with the conventional ones with the same Si content. Although details of the mechanism by which the surfactant alters the silicon substitution mechanism are yet to be studied, it is proposed that the electrostatic interaction between the positively charged surfactant (the fatty amines are also protonated at the low synthesis pH) and the negatively charged framework is the main driving force (Figure 1.10).

Additionally, it was found that the microemulsion method led to the generation of very small crystallites that are about 100 nm for SAPO-34 [42] and also to a substantial increase in the mesopore surface and volume. For this CHA-type material, the $V_{\text{micro}}/V_{\text{total}}$ ratio was found to be 0.34 as compared with the reference sample synthesized in the aqueous phase (0.47).

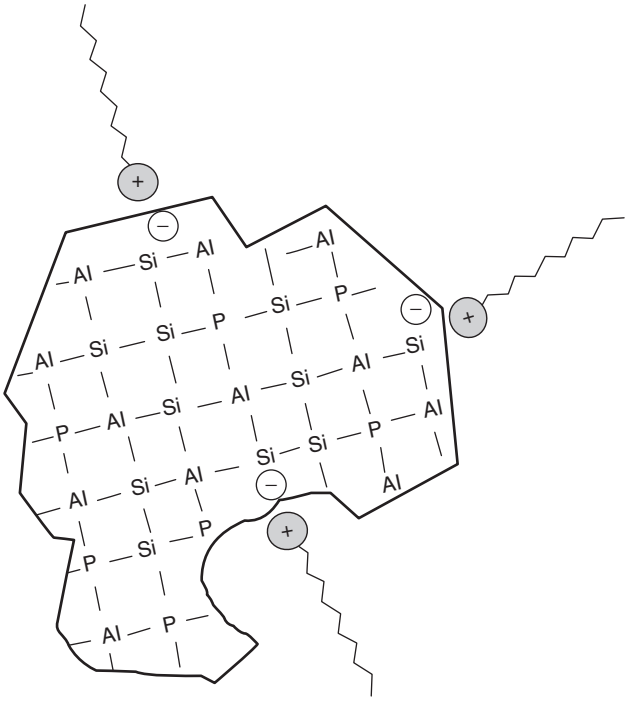

Figure 1.10 Schematic illustration of the crystal of the SAPO-type material prepared using two-liquid phases in the synthesis gel in the presence of positively charged surfactant.

1.3.3
Synthesis in the Presence of Pore-Forming Agents

One of the simplest methods to create mesopore-sized holes inside the zeolite crystals is to use a matrix, or pore-imprinting template, that can be easily removed after crystallization, most preferably in the same air-calcination step that is usually required to eliminate the structure-directing agent (SDA) occluded inside the zeolite micropores. Jacobsen *et al.* [23] reported such a method as an extension of the confined space synthesis described earlier. By impregnating the carbon black pearls used as a confining agent with an excess of the synthesis gel, ZSM-5 crystals containing embedded carbon particles are obtained. After air calcination, the carbon is burned off, leaving the zeolite crystals permeated by the pores (Figures 1.7 and 1.11).

This method has been extended to the synthesis of other zeolite structures such as MEL, BEA, MTW, AFI, and CHA; and other carbon sources such as carbon nanotubes or nanofibers [43, 44], ordered mesoporous carbons [45], and carbon aerogels [46, 47]. Some of the other approaches involve the use of polymeric organic materials that can play a role similar to that of carbon, which are pyrolyzed and, finally, burned off during calcination.

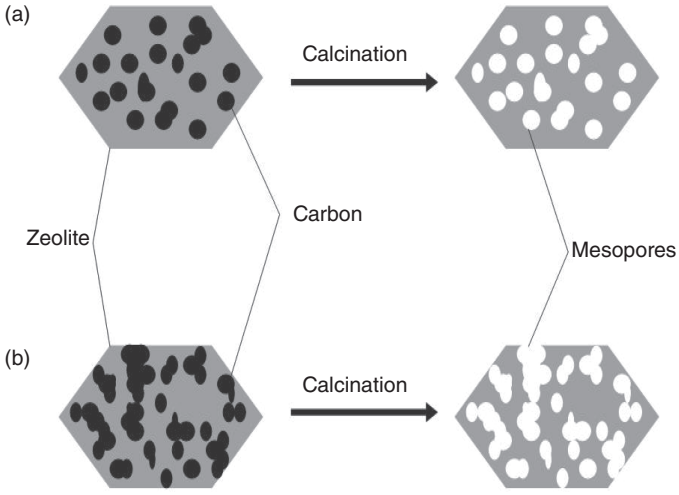

Figure 1.11 Schematic illustration of the pores created inside the crystals. In (a), the mesopores formed are not accessible from the external surface of the crystals, whereas in (b), some of the pores are accessible.

Several aspects of these synthesis methods are worth mentioning in this chapter. First, as it has already been noticed in Ref. [36], many of the mesopore zeolite materials obtained exhibit a noticeable reduction in the micropore volume as compared with the conventional ones, which implies partial amorphization of the samples during calcination. This effect is not surprising, owing to the expected increase in the temperature at the interface between the carbon particles and the zeolite surface, where the actual temperature during the exothermic burning of the carbon would be much higher than the one recorded at the bulk, unless special precautions are taken to avoid such undesirable effect.

Other important aspects to be discussed are concerned with the actual accessibility of the pores created inside the crystals by the aforementioned procedures to the reactants molecules. Figure 1.11 depicts the general representation of the formation of mesopores holes using pore-imprinting carbons or carbon precursors. As shown in Figure 1.11a, there is a thin slice of the inner part of the crystal where most of the mesopores are not be accessible from the external surface of the crystals. In the situation represented in Figure 1.11b, some of the pores are accessible. The method generally used to determine the mesoporosity of these materials is nitrogen adsorption; however, it does not provide information on the actual accessibility of bulky molecules, that is, molecules of size greater than the micropore size. Mercury porosimetry is a convenient technique to determine the effective accessibility and interconnection of the mesopores present inside the crystals, although it is limited to pores of size above 4 nm while using conventional instruments, which is much smaller than the diameters of many pores reported for these materials. Although the use of this technique has already been recommended [48],

it is surprising to see how scarcely it has been used in the textural characterization of mesoporous zeolites, as concluded from the data reported in the available scientific literature. In the absence of this technique or any other suitable technique used to determine the effective accessibility of the inner mesopores to bulky molecules, little can be concluded on the success of these approaches to accomplish the initial goal, that is, to enhance the access of large reactant molecules to the active sites located inside the micropores.

The effective growth of the zeolite crystals around the pore-forming agents, as the carbon particles, should be based on the existence of an appropriate chemical interaction between the carbon particles and the oligomeric aluminosilicate present in the synthesis medium. However, it can be determined from the published literature that little attention has been generally paid to the eventual modification of this interaction in order to influence the textural properties of the resulting hierarchical material. This aspect seems to reflect the predominance of the experimental approaches in which the pore-imprinting ability of the pore-forming agents is seen as a "ball dipped on fresh concrete" model, where the zeolite is considered just an inert receptacle for the "hard spheres" of carbon particles. On the contrary, chemical approaches can aid in designing new materials with enhanced pore accessibility.

The surface of the carbon materials used as a mesopore template contains chemical groups such as OH and C=O. This is schematically represented in Figure 1.12 for carbon aerogels obtained by pyrolization of formaldehyde–resorcinol organic aerogels [49, 50]. Moreover, the carbon aerogels can be chemically activated by the oxidizing agents, and in this way, high-density surface oxide functional groups

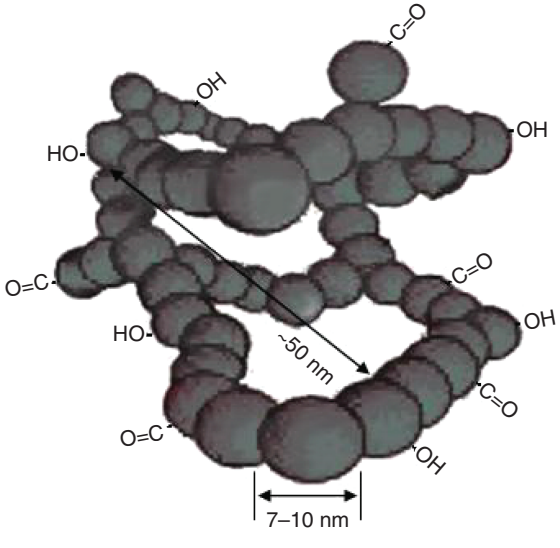

Figure 1.12 Schematic illustration of the surface of the carbon aerogel. (*Source*: Adapted from *http://www.reade.com/western-region-%28usa%29/8826*.)

are obtained, thereby altering the polar character of the carbon surface [51, 52]. Therefore, the interaction between the carbon particles and the zeolite precursors can be regulated as a function of the surface chemistry of carbon. Moreover, this interaction is pH dependent; therefore, it would most probably be different for the synthesis of zeolite in alkaline media as compared with the crystallization of AlPO-type materials, which usually takes place at neutral–acidic pH values. Following this approach, the chemical nature of the zeolite–carbon interface could, eventually, also affect the chemical properties of the zeolite surface, particularly the concentration and location of the acid sites. This aspect is of key importance in obtaining a catalytically active mesoporous surface using the aforementioned pore-imprinting techniques.

1.4 Postsynthesis Methodologies

A large number of different strategies have been developed to improve the pore accessibility in preformed zeolite crystals, which are grouped as postsynthesis methodologies in this chapter. Some of these strategies are based on the existence of marked anisotropies in the starting materials, either in their crystal growth habit and morphology, or in the preferential location of specific T atoms at specific T sites, or both. In other approaches, the zeolite crystals are subjected to certain chemical treatments, which, in some cases, involve partial recrystallization of the zeolite, in order to create mesoporosity in the crystal bulk. These different approaches are separately discussed next.

1.4.1 Materials with High Structural Anisotropy: Layered Zeolites

As discussed earlier, a successful strategy to gain micropore accessibility is to decrease the crystal size. For zeolite materials that exhibit a large structural anisotropy, that is, where the crystal growth is most favored in a particular direction, this strategy enables the synthesis of layered zeolite materials, which are seen as "bidimensional" or 2D materials, in contrast to the tridimensional (3D) and more conventional zeolite structures [53].

In a simplified manner and with regard to the crystal habit formalism, these 2D materials can be seen as extended platelets of the type represented in Figure 1.6. It can be seen that, in contrast to 3D crystals, the platelet thickness should be well below 10–20 nm in order to have a significant external area. However, it can be seen that, in addition to this beneficial effect, in some cases the layered materials facilitate the access of bulky molecules to the active sites that could be essentially inaccessible in the corresponding 3D structures.

There are several layered zeolite precursors, which can be seen as stacked zeolite layers containing the zeolite template occluded in the interlayer space, as shown in Figure 1.13. The interlayer interaction is relatively weak, in such a way that these

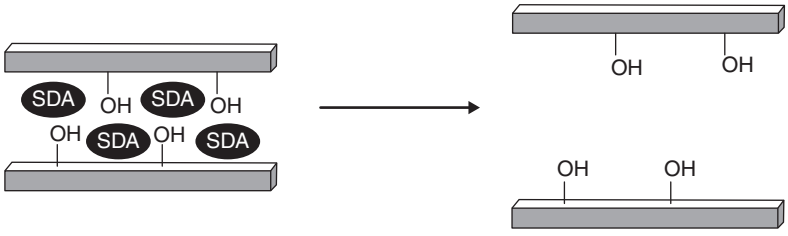

Figure 1.13 A simplified representation of a 2D material. The interlayer interaction is weak, and delamination is possible with an appropiate treatment.

precursors can be subjected to appropriate swelling and delamination treatments in order to obtain lamellar materials with a very small thickness. This is the chemical disassembling pathway, which is included in Scheme 1.1. The first successful example of these methodologies for obtaining 2D zeolite materials was the synthesis of the material denoted ITQ-2, which was obtained from the layered zeolite precursor MCM-22 (P) using hexadecyltrimethylammonium bromide (CTAB) as a swelling agent [54]. A very interesting feature of this approach is that this method not only led to the production of a high-surface material, but also, more importantly, enabled free access to the zeolite supercages that would otherwise be accessible only from the 10 rings in the fully condensed 3D MCM-22 structure, which imparted specific catalytic properties to the resulting material.

Layered precursors of zeolite FER [55] and Nu-6 [56] are also known. It can be seen in Figure 1.13 that the lamella comprising these materials are terminated by the Si–OH groups, which, under appropriate conditions, could undergo condensation to give rise to 3D structures.

Recently, a somewhat different approach for the synthesis of 2D materials has been reported [57, 58], which involves selective removal of atoms of specific reactive elements located at specific structural T sites. The Ge atoms at specific interlayer positions can be removed without dissolving the Si or Al atoms, and in this way, lamellar materials are obtained (Figure 1.14). Although it is beyond the scope of this study, it is worth mentioning that these individual lamellar materials can undergo rearrangement through condensation of the Si–OH present at the surface, thereby giving rise to new zeolite topologies [59].

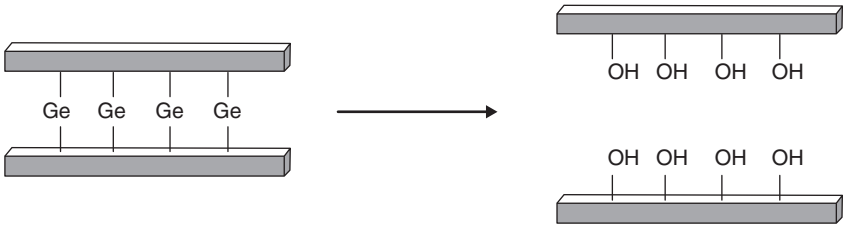

Figure 1.14 Selective removal of atoms of certain reactive elements (in this case, Ge) located at specific structural T sites.

It can be summarized that, although the preparation of 2D zeolite materials has experienced a significant development in recent years, the available methods are applicable only to a limited variety of structures.

1.4.2 Removal/Reorganization of T Atoms in the Crystal Bulk

Dealumination treatments of zeolite faujasite are commonly used to obtain faujasite materials with higher Si/Al ratio, which are more stable and possess stronger acidity as compared with the untreated ones. During these treatments, mesopores are also formed [60]. Although dealumination is highly optimized for FAU, it cannot be generally extended to other zeolite materials. Moreover, as Al extraction occurs during dealumination, the acidity of the final material is also strongly affected. For zeolites already having high Si/Al, further dealumination does not increase the acid strength of the remaining acid sites and decreases their concentration, with little benefit, if any, for catalysis.

Selective removal of silicon from zeolite, or desilication, was highly explored in the past decade as a promising method to create mesopores inside the zeolite crystals with different structures. This method was introduced by Ogura *et al.* [61] and applied to ZSM-5, and it involves the treatment of the zeolite with a NaOH solution. Although mesoporosity is achieved, a marked decrease in the micropore volume is observed, in addition to a high loss of the crystal mass, which is only partially dissolved. Some amount of aluminum is also removed, however, to much less extent as compared with silicon, which results in an overall decrease of Si/Al in the treated zeolite.

The drawbacks of the desilication strategy were soon recognized, and several strategies have been developed over the years to overcome such problems and extend the methodology to zeolites with different structures and Si/Al ratios. The basic strategy of these approaches involves moderation of the intensity of silicon removal observed when strong alkaline solutions of inorganic cations are the only attacking reactants used. Some of them are briefly mentioned in this chapter.

It has been observed that the dissolution of silicon in as-made zeolites still containing the template is much lower than that found in the calcined materials [62]. Further, the template protects the Si–O–Si network from excessive and massive leaching by the alkaline solution. Inspired by this observation, Pérez-Ramirez *et al.* [63] controlled the calcination of the as-made zeolite Beta in order to remove the template only partially, which enables control of the desilication process. Furthermore, a somewhat related strategy reported by the same group [36] involves treatment of the zeolite with NaOH solution in the presence of quaternary ammonium cations that act as pore-growth moderators.

A method for creating mesopore zeolite crystals by avoiding the loss of material and by simultaneously preserving the zeolite structure in its integrity has been reported recently [64–67]. In addition to being used for the treatment of the zeolite, FAU, this method has been claimed to be applicable to other structures as well, such as mordenite, ZSM-5, A, and X, with a solution of the surfactant CTAB

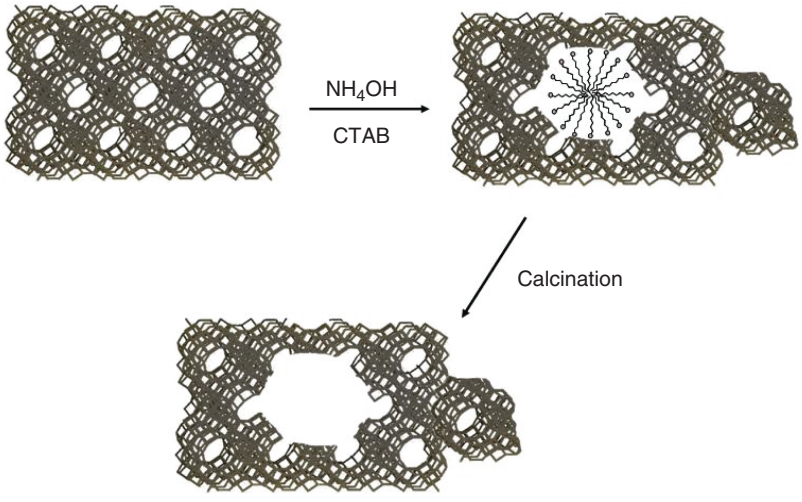

Figure 1.15 Schematic illustration of the mesopore zeolite formation process in the presence of a surfactant.

in aqueous NH_4OH or TMAOH (tetramethylammonium hydroxide) at 150 °C. A more detailed and ample discussion of this strategy is given in Ref. [67]. The pore size distribution of the mesopores created in this way inside the FAU crystals is very narrow and centered at 4 nm, which is quite similar to that of the ordered mesoporous materials MCM-41 obtained using this surfactant, although there is no evidence on the existence in the treated materials of a separate mesoporous phase. Figure 1.15 shows a simple scheme of the resulting materials, where the surfactant micelles form inside the crystals, leading to the formation of mesopores after calcination. Almost 100% of the initial zeolite weight has been recovered after the treatment, and no separate mesoporous phase has been detected so far. The formation of mesopores, as explained by these authors, is the result of recrystallization of the zeolite. This conclusion is rather surprising from the point of view of the existing knowledge of the gel composition and temperature required to crystallize FAU, and it would be interesting to further explore the recrystallization mechanism that enables the formation of such mesoporous FAU crystals by this surfactant-assisted approach. The mesopore FAU zeolite synthesized using this strategy shows improved performance in fluid catalytic cracking (FCC) at commercial scale [67].

1.5 Conclusions

In recent years, significant progress has been made to enhance the accessibility of bulky molecules to the interior of the micropores of zeolite materials. According

to the existing knowledge, some of the approaches work better for certain zeolite structures, and apparently, a general method has yet to be found. However, already there are quite a large number of methods available for most of the zeolite materials that are of commercial interest.

Many of these methods led to the production of materials that exhibit a large mesopore surface, quite similar, in many cases, to the external surface of ultrasmall zeolite crystals, and it would be interesting to know whether or not the stability and surface chemical properties of both set of materials are related. This has led to a more general question that is yet to be answered: to what extent does the method used to enhance the microporosity accessibility modify the nature of the active sites present at the zeolite surface, in addition to the stability of these sites, and that of the whole crystal? It would be quite useful, in this regard, to determine the surface acidity of the mesopore (external) surface in a systematic and selective way. This aspect has been considered in several of the following chapters of this volume, more specifically in Chapter 16.

The alleviation of the restrictions on the diffusion of reactants to penetrate the interior of the micropore system is obviously at the bottom of all these strategies; however, surprisingly, very few works have determined the actual interconnection between the mesopores created by these methods. The simple presence of mesopores inside the crystals does not necessarily translate itself into an automatic benefit for the diffusion of ingoing molecules, if access to them is provided through the zeolite micropores, that is, if there is no actual connectivity among the mesopores. Systematic studies on molecular transport in mesoporous zeolites are required in order to shed light on this critical aspect of the field, which is explored in Chapter 13 and, more specifically, also in Chapter 14.

Acknowledgments

The authors acknowledge Dr Carlos Márque-Álvarez for providing Figure 1.6. The financial support from MINECO (Spain) through the project MAT2012-31127 is greatly appreciated.

References

1. Schlenker, J.L. and Kühl, G.H. (1993) in *Proceedings of the 9th International Zeolite Conference*. (eds R. von Ballmoos, J.B. Higgins, and M.M. Treacy), vol. I, Butterworth-Heinemann, Boston, pp. 3–9.
2. Bartow, V. (1953) Axel Fredrik Cronstedt, *J. Chem. Educ.*, **30**, 247–252.
3. Barrer, R.M. (1938) The Sorption of polar and non-polar gases by zeolites. *Proc. R. Soc. London*, **167**, 392–420.
4. Wise, W.S. (2013) in *Handbook of Natural Zeolites* (ed C. Colella), De Freded Editore.
5. Derouane, E.G. (1982) in *Intercalation Chemistry* (eds M.S. Whitthinham and A.J. Jacobsen), Academic Press, New York, p. 101.
6. Bellusi, G., Carati, A., and Millini, R. (2010) in *Synthesis, Reactions and Application*, vol. 2 (eds J. Cejka and A. Corma), Wiley-VCH Verlag GmbH, Weinheim, pp. 449–491.

7. Čejka, J., Centi, G., Pérez-Pariente, J., and Roth, W.J. (2012) Zeolite-based materials for novel catalytic applications: opportunities, perspectives and open problems. *Catal. Today*, **179** (1), 2–15.
8. (a) Baerlocher, C., McCusker, L.B., and Olson, D.H. (2007) *Atlas of Zeolite Framework Types*, 6th edn, Elsevier; (b) IZA-SC *www.iza-structure.org/databases/* (accessed 20 August 2014).
9. Bellussi, G., Carati, A., Rizzo, C., and Millini, R. (2013) New trends in the synthesis of crystalline microporous materials. *Catal. Sci. Technol.*, **3** (4), 833–857.
10. Brunner, G.O. and Meier, W.M. (1989) Framework density distribution of zeolite-type tetrahedral nets. *Nature*, **337** (6203), 146–147.
11. Corma, A., Navarro, M.T., Rey, F., Rius, J., and Valencia, S. (2001) Pure polymorph C of zeolite beta synthesized by using framework isomorphous substitution as a structure-directing mechanism. *Angew. Chem. Int. Ed.*, **40** (12), 2277–2280.
12. Corma, A., Díaz Cabañas, M.J., Jorda, J.L., Martinez, C., and Moliner, M. (2006) High-throughput synthesis and catalytic properties of a molecular sieve with 18- and 10- member rings. *Nature*, **443** (7113), 842–845.
13. Jiang, J., Jorda, J.L., Diaz-Cabañas, M.J., Yu, J., and Corma, A. (2010) The synthesis of an extra-large-pore zeolite with double three-ring building units and a low Framework density. *Angew. Chem. Int. Ed.*, **49** (29), 4986–4988.
14. Corma, A., Diaz-Cabañas, M.J., Jiang, J., Afeworki, M., Dorset, D.L., Soled, S.L., and Strohmaier, K.G. (2010) Extra-large pore zeolite (ITQ-40) with the lowest framework density containing double four- and double three- rings. *Proc. Natl. Acad. Sci. U.S.A.*, **107** (32), 13997–14002.
15. Millini, R. (2013) Zeolites in the refining and petrochemical industries: future perspectives. 5th Czech-Italian-Spanish Conference on Molecular Sieves and Catalysis, June 16–19, PL-1.
16. Tosheva, L. and Valtchev, V.P. (2005) Nanozeolites: synthesis, crystallization mechanisms, and applications. *Chem. Mater.*, **17**, 2494–2513.
17. Mintova, S., Gilson, J.-P., and Valtchev, V. (2013) Advances in nanosized zeolites. *Nanoscale*, **5**, 6693–6703.
18. Ng, E.-P., Chateigner, D., Bein, T., Valtchev, V., and Mintova, S. (2012) Capturing ultrasmall EMT zeolite from template-free systems. *Science*, **335** (6064), 70–73.
19. Van Heyden, H., Mintova, S., and Bein, T. (2008) Nanosized SAPO-34 synthesized from colloidal solutions. *Chem. Mater.*, **20**, 2956–2963.
20. Madsen, C. and Jacobsen, C.J.H. (1999) Nanosized zeolites crystals-Convenient control of crystal size distribution by confined space synthesis. *Chem. Commun.*, **8**, 673–674.
21. Jacobsen, C.J.H., Madsen, C., and Schmidt, I. (2000) Confined space synthesis. A novel route to nanosized zeolites. *Inorg. Chem.*, **39** (11), 2279–2283.
22. Jacobsen, C.J.H., Madsen, C., Janssens, V.W., Jakobsen, H.J., and Skibsted, J. (2000) Zeolites by confined space synthesis. Characterization of the acid sites in nanosized ZSM-5 by ammonia desorption and $^{27}Al/^{29}Si$-MAS NMR spectroscopy. *Microporous Mesoporous Mater.*, **39** (1-2), 393–401.
23. Jacobsen, C.J.H., Madsen, C., Houzvicka, J., Schmidt, I., and Carlsson, A. (2000) Mesoporous zeolite single crystals. *J. Am. Chem. Soc.*, **122**, 7116–7117.
24. Wang, M.-X., Liu, Q., Sun, H.-f., Ogbeifun, N., Xu, F., Stach, E.A., and Xie, J. (2010) Investigation of carbon corrosion in polymer electrolyte fuel cells using steam etching. *Mater. Chem. Phys.*, **123**, 761–766.
25. Wang, H., Liao, X.Z., Jiang, Q.Z., Yang, X.W., He, Y.S., and Ma, Z.F. (2012) A novel $Co(phen)_2/C$ catalyst for the oxygen electrode in rechargeable lithium air batteries. *Chin. Sci. Bull.*, **57** (16), 1959–1963.
26. Kim, S.-S., Shah, J., and Pinnavaia, T.J. (2003) Colloidal-imprinted carbons as templates for the nanocasting synthesis of mesoporous ZSM-5 zeolite. *Chem. Mater.*, **15** (8), 1664–1668.

27. Serrano, D.P., Aguado, J., Escola, J.M., Rodríguez, J.M., and Peral, A. (2006) Hierarchical zeolites with enhanced textural and catalytic properties synthesized from organofunctionalized seeds. *Chem. Mater.*, **18** (10), 2462.
28. Serrano, D.P., Aguado, J., Escola, J.M., and Pizarro, P. (2013) Synthesis strategies in the search for hierarchical zeolites. *Chem. Soc. Rev.*, **42**, 4004–4035.
29. Serrano, D.P., Aguado, J., Morales, G., Rodríguez, J.M., Peral, A., Thommes, M., Epping, J.D., and Chmelka, B.F. (2009) Molecular and meso- and macroscopic properties of hierarchical nanocrystalline ZSM-5 zeolite prepared by seed silanization. *Chem. Mater.*, **21** (4), 641–654.
30. Wang, H. and Pinnavaia, T.J. (2006) MFI zeolite with small and uniform intracrystal mesopores. *Angew. Chem. Int. Ed.*, **45** (45), 7603–7606.
31. Park, D.H., Kim, S.S., Wang, H., Pinnavia, T.J., Papapetrou, M.C., Lappas, A.A., and Triantafyllidis, K.S. (2009) Selective petroleum refining over a zeolite catalyst with small intracrystal mesopores. *Angew. Chem. Int. Ed.*, **48** (41), 7645–7648.
32. Camblor, M.A., Corma, A., Martínez, A., Mocholí, F.A., and Pérez-Pariente, J. (1989) Benefits in activity and selectivity of small Y zeolite crystallites stabilized by a higher silicon-to-aluminium ratio by synthesis. *Appl. Catal.*, **55**, 65–74.
33. Serrano, D.P., García, R.A., Vicente, G., Linares, M., Procházkova, D., and Cejka, J. (2011) Acidic and catalytic properties of hierarchical zeolites and hybrid ordered mesoporous materials assembled from MFI protozeolitic units. *J. Catal.*, **279** (2), 366–380.
34. Serrano, D.P., Aguado, J., Escola, J.M., Rodríguez, J.M., and Peral, A. (2010) Catalytic properties in polyolefin cracking of hierarchical nanocrystalline HZSM-5 samples prepared according to different strategies. *J. Catal.*, **276** (1), 152–160.
35. Serrano, D.P., García, R.A., Linares, M., and Gil, B. (2012) Influence of the calcination treatment on the catalytic properties of hierarchical ZSM-5. *Catal. Today*, **179** (1), 91–101.
36. Pérez-Ramirez, J., Verboekend, D., Bonilla, A., and Abelló, S. (2009) Zeolites catalysts with tunable hierarchy factor by pore-growth moderators. *Adv. Funct. Mater.*, **19**, 3972–3979.
37. Derouane, E.G., Valyocsik, E.W., and Von Balmoos, R. (1984) Synthesis of Silicophosphoaluminate US Patent 0,146, 384.
38. Montoya-Urbina, M., Cardoso, D., Pérez-Pariente, J., Sastre, E., Blasco, T., and Fornés, V. (1998) Characterization and catalytic evaluation of SAPO-5 synthesized in aqueous and two-liquid phase medium in presence of a cationic surfactant. *J. Catal.*, **173**, 501–510.
39. Franco, M.J., Mifsud, A., and Pérez-Pariente, J. (1995) Study of SAPO-5 obtained from surfactant-containing gels: part 1. Crystallization parameters and mechanism of Si substitution. *Zeolites*, **15** (2), 117–123.
40. Del Val, S., Blasco, T., Sastre, E., and Pérez-Pariente, J. (1995) Synthesis of SiVPI-5 with enhanced activity in acid catalysed reactions. *J. Chem. Soc., Chem. Commun.*, 731–732.
41. Blasco, T., Chica, A., Corma, A., Murphy, W., Agundez-Rodríguez, J., and Pérez-Pariente, J. (2006) Changing the Si distribution in SAPO-11 by synthesis with surfactants improves the hydroisomerization/dewaxing properties. *J. Catal.*, **242**, 153–161.
42. Álvaro-Muñoz, T., Márquez-Álvarez, C., and Sastre, E. (2013) Enhanced stability in the methanol-to-olefins process shown by SAPO-34 catalyst synthesized in biphasic medium. *Catal. Today*, **215**, 208–215.
43. Janssen, J., Scmidt, I., Jacobsen, C.J.H., Koster, A.J., and De, K.P. (2003) Exploratory study of mesopore templating with carbon during zeolite synthesis. *Microporous Mesoporous Mater.*, **65**, 59–75.
44. Schmidt, F., Paasch, S., Brunner, E., and Kaskel, S. (2012) Carbon templated SAPO-34 with improved adsorption kinetics and catalytic performance in the MTO –reaction. *Microporous Mesoporous Mater.*, **164**, 214–221.

45. Yang, Z., Xia, Y., and Mokaya, R. (2004) Zeolite ZSM-5 with unique supermicropores synthesized using mesoporous carbon as template. *Adv. Mater.*, **16** (8), 727–732.
46. Tao, Y., Kanoh, H., and Kaneko, K. (2003) ZSM-5 monolith of uniform mesoporous channels. *J. Am. Chem. Soc.*, **125** (20), 6044–6045.
47. Tao, Y., Kanoh, H., Abrams, L., and Kaneko, K. (2006) Mesopore-modified zeolites: preparation, characterization and applications. *Chem. Rev.*, **106** (3), 896–910.
48. Egeblad, K., Christensen, C.H., Kustova, M., and Christensen, C.J.H. (2008) in *Zeolites: From Model Materials to Industrial Catalysts* (eds J. Cejka, J. Pérez-Pariente, and W.J. Roth), Transworld Research Network, pp. 391–422.
49. Pekala, R.W. and Alviso, C.T. (1992) Carbon aerogels and xerogels. *MRS Proc.*, **270**, 3.
50. Zapata-Benabithe, Z., Carrasco-Marín, F., De Vicente, J., and Moreno-Castilla, C. (2013) Carbon aerogel microspheres and monoliths from resorcinol-formaldehyde mixtures with varying dilution ratios: preparation, surface characteristics, and electrochemical double-layer capacitances. *Langmuir*, **29** (20), 6166–6173.
51. Elkhatat, A.M. and Al-Muhtaseb, S.A. (2011) Advances in tailoring resorcinol-formaldehyde organic and carbon gels. *Adv. Mater.*, **23** (26), 2887–2903.
52. Hwangh, S.W. and Hyun, S.H. (2004) Capacitance control of carbon aerogel electrodes. *J. Non Cryst. Solids*, **347** (1-3), 238–245.
53. Solânea, F., Ramos, O., de Pietre Mendelssom, K., and Pastore, H.O. (2013) Lamellar zeolites: an oxymoron? *RSC Adv.*, **3**, 2084–2111.
54. Corma, A., Fornes, V., Pergher, S.B., Maesen, T.L.M., and Buglass, J.G. (1998) Delaminated zeolite precursors as selective acidic catalysts. *Nature*, **396** (6709), 353–356.
55. Perego, G., Bellussi, G., Millini, R., Alberti, A., and Zanardi, S. (2002) B-containing molecular sieves crystallized in the presence of ethylenediamine. Part I: crystal structure of as-synthesized B-FER. *Microporous Mesoporous Mater.*, **56** (2), 193–202.
56. Zanardi, S., Alberti, A., Cruciani, G., Corma, A., Fornés, V., and Bruneli, M. (2004) Crystal structure determination of zeolite Nu-6 (2) and its layered precursor Nu-6 (1). *Angew. Chem. Int. Ed.*, **43** (37), 4933–4937.
57. Roth, W.J., Shvets, O.V., Shamzhy, M., Chlubná, P., Kubu, M., Nachtigall, P., and Cejka, J. (2011) Postsynthesis transformation of three-dimensional framework into a lamellar zeolite with modifiable architecture. *J. Am. Chem. Soc.*, **133**, 6130–6133.
58. Chlubná, P., Roth, W.J., Greer, H.F., Zhou, W., Shvets, O., Zukal, A., Cejka, J., and Morris, R.E. (2013) 3D to 2D routes to ultrathin and expanded zeolitic materials. *Chem. Mater.*, **25** (4), 542–547.
59. Roth, W.J., Nachtigall, P., Morris, R.E., Wheatley, P.S., Seymour, V.R., Asbrook, S.E., Chlubná, P., Grajciar, L., Polozij, M., Zukal, A., Shvets, O., and Cejka, J. (2013) A family of zeolites with controlled pore size prepared using a top-down method. *Nat. Chem.*, **5** (7), 628–633.
60. Martens, J.A., Grobet, P.J., and Jacobs, P.A. (1991) The chemistry of the dealumination of faujasite zeolites with silicon tetrachloride. *Stud. Surf. Sci. Catal.*, **63**, 355–379.
61. Ogura, M., Shinomiya, S.Y., Tateno, J., Nara, Y., Kikuchi, E., and Matsukata, M. (2000) Formation of uniform mesopores in ZSM-5 zeolite through treatment in alkaline solution. *Chem. Lett.*, (8), 882–883.
62. Cizmek, A., Subotic, B., Smit, I., Tonejc, A., Aiello, R., Crea, F., and Nastro, A. (1997) Dissolution of high-silica zeolites in alkaline solutions II. Dissolution of "activated" silicalite-1 and ZSM-5 with different aluminum content. *Microporous Mesoporous Mater.*, **8** (3-4), 159–169.
63. Pérez-Ramirez, J., Abelló, S., Bonilla, A., and Groen, J.C. (2009) Tailored mesoporosity development in zeolites crystals by partial detemplation and desilication. *Adv. Funct. Mater.*, **16**, 164–172.
64. Ying, J.Y. and García-Martínez, J. (2009) Cracking catalysts. US Patent 7, 589,041.

65. García-Martínez, J., Johnson, M., Valla, J., and Li, K. (2012) Mesostructured zeolite Y-high hydrothermal stability and superior FCC catalytic performance. *Catal. Sci. Technol.*, **2**, 987–994.
66. García-Martínez, J., Li, K., and Krishnaiah, G. (2012) A mesostructured Y zeolite as a superior FCC catalyst-from lab to refinery. *Chem. Commun.*, **48**, 11841–11843.
67. Li, K., Valla, J., and García-Martínez, J. (2014) Realizing the commercial potential of hierarchical zeolites: new opportunities in catalytic cracking. *ChemCatChem*, **6**, 46–66.